Phosphorylation of Nephrin Triggers Ca²⁺ Signaling by Recruitment and Activation of Phospholipase C-γ1*

Yutaka Harita[‡§], **Hidetake Kurihara**[¶], **Hidetaka Kosako**[‡], **Tohru Tezuka**[∥], **Takashi Sekine**[§], **Takashi Igarashi**[§], **Ikuroh Ohsawa**[**], **Shigeo Ohta**[**], and **Seisuke Hattori**[‡ ‡‡1]

*From the ‡Division of Cellular Proteomics (BML) and ∥Department of Oncology, Institute of Medical Science, University of Tokyo, 4-6-1 Shirokanedai, Minato-ku, Tokyo 108-8639, Japan, the §Department of Pediatrics, Graduate School of Medicine, University of Tokyo, 7-3-1 Hongo, Bunkyo-ku, Tokyo 113-8655, Japan, the ¶Department of Anatomy, Juntendo University School of Medicine, 2-1-1 Hongo, Bunkyo-ku, Tokyo 113-8421, Japan, the **Department of Biochemistry and Cell Biology, Institute of Development and Aging Sciences, Graduate School of Medicine, Nippon Medical School, Tokyo 113-8602, Japan, and the ‡‡Department of Biochemistry, School of Pharmaceutical Sciences, Kitasato University, 5-9-1 Shirokane, Minato-ku, Tokyo 108-8641, Japan*

A specialized intercellular junction between podocytes, known as the slit diaphragm (SD), forms the essential structural framework for glomerular filtration in the kidney. In addition, mounting evidence demonstrates that the SD also plays a crucial role as a signaling platform in physiological and pathological states. Nephrin, the major component of the SD, is tyrosine-phosphorylated by a Src family tyrosine kinase, Fyn, in developing or injured podocytes, recruiting Nck to Nephrin via its Src homology 2 domain to regulate dynamic actin remodeling. Dysregulated Ca²⁺ homeostasis has also been implicated in podocyte damage, but the mechanism of how podocytes respond to injury is largely unknown. Here we have identified phospholipase C-γ1 (PLC-γ1) as a novel phospho-Nephrin-binding protein. When HEK293T cells expressing a chimeric protein consisting of CD8 and Nephrin cytoplasmic domain (CD) were treated with anti-CD8 and anti-mouse antibodies, clustering of Nephrin and phosphorylation of Nephrin-CD were induced. Upon this clustering, PLC-γ1 was bound to phosphorylated Nephrin Tyr-1204, which induced translocation of PLC-γ1 from cytoplasm to the CD8/Nephrin cluster on the plasma membrane. The recruitment of PLC-γ1 to Nephrin activated PLC-γ1, as detected by phosphorylation of PLC-γ1 Tyr-783 and increase in inositol 1,4,5-trisphosphate level. We also found that Nephrin Tyr-1204 phosphorylation triggers the Ca²⁺ response in a PLC-γ1-dependent fashion. Furthermore, PLC-γ1 is significantly phosphorylated in injured podocytes *in vivo*. Given the profound effect of PLC-γ in diverse cellular functions, regulation of the Ca²⁺ signaling by Nephrin may be important in modulating the glomerular filtration barrier function.

The glomerular capillary wall of the kidney functions as a highly selective filtration barrier that retains albumin and other plasma proteins in the circulation (1). A defect in glomerular ultrafiltration results in several forms of congenital or acquired kidney diseases, which is typically manifested by a massive loss of protein in the urine (proteinuria), which is key symptom of nephrotic syndrome (2). The glomerular capillary wall consists of three structural layers: a layer of a fenestrated endothelial cells, the glomerular basement membrane, and the visceral epithelial cells, also called podocytes. Podocytes form primary processes that further extend numerous elaborate foot processes. Foot processes from neighboring podocytes interdigitate with each other and surround the entire surface of capillary loops. These foot processes are bridged by a unique cell adhesion structure, the slit diaphragm (SD).[2]

Over the last decade, mutations in genes encoding the SD proteins have been identified in several forms of congenital nephrotic syndrome (2). The first of these molecules to be identified was Nephrin (3). Nephrin is a membrane-spanning glycoprotein encoded by the *NPHS1* gene and is a member of the immunoglobulin superfamily. Nephrin is specifically expressed in glomerular podocytes, and mutations in *NPHS1* cause heavy proteinuria before birth and result in early death (congenital nephrotic syndrome of the Finnish type) (4). Several other molecules, including Neph1 (5), podocin (6), FAT1 (7), and CD2-associated protein (8) have been identified as components of SD, and genetic disruption of these molecules in human diseases or in genetically manipulated mice results in similar phenotypic conditions: a flattening (effacement) of foot processes, loss of SD, and proteinuria. The identification of these SD components has shed light on the pathogenesis of proteinuria and emphasized the critical role of SD in maintaining the function of the glomerular filtration barrier.

In addition to its role as a structural framework of the filtration barrier, SD has been implicated in podocyte intracellular signaling (9). Nephrin interacts with phosphatidylinositol 3-kinase p85, which leads to increased Akt activity and a reduction in cell death induced by apoptotic stimuli (10). SD components are also modulated by tyrosine phosphorylation. The cytoplas-

[1] To whom correspondence should be addressed: Division of Cellular Proteomics (BML), Institute of Medical Science, University of Tokyo, 4-6-1 Shirokanedai, Minato-ku, Tokyo 108-8639, Japan. Fax: 81-3-6409-2073; E-mail: hattoris@ims.u-tokyo.ac.jp.

[2] The abbreviations used are: SD, slit diaphragm; PLC, phospholipase C; CD, cytoplasmic domain; SH2, Src homology 2; GFP, green fluorescent protein; GST, glutathione S-transferase; PS, protamine sulfate; IP₃, inositol 1,4,5-trisphosphate; PBS, phosphate-buffered saline; MALDI-TOF, matrix-assisted laser desorption ionization time-of-flight.

mic domain (CD) of Nephrin is transiently tyrosine-phosphorylated by a Src family tyrosine kinase, Fyn, in developing or injured podocytes (11, 12). The Src homology 2 domain of Nck binds to several phosphorylated tyrosines of Nephrin, and this interaction regulates actin polymerization (12, 13), indicating a dynamic regulatory role of Nephrin in the podocyte cytoskeleton. The critical role of tyrosine phosphorylation in filtration barrier function is also suggested by proteinuria and the effacement of foot processes in *fyn*-deficient mice (11, 14).

New insights have recently emerged concerning the functional importance of Ca^{2+} signaling in the pathophysiology of podocyte. Mutant forms of canonical TRPC6 (transient receptor potential cation channel 6) have been shown to cause congenital proteinuria (15). TRPC6 is a Ca^{2+}-permeable cation channel activated following stimulation of membrane receptors linked to PLC. TRPC6 is highly expressed in podocytes and closely localized to the SD. Some mutants found in patients are gain-of-function mutations, leading to speculation that the exaggerated Ca^{2+} signaling disrupts glomerular cell function (15, 16). But to date, the mechanism by which Ca^{2+} signaling is associated with glomerular pathogenesis is largely unknown.

In the present study, we identified PLC-γ1 as a novel phospho-Nephrin-binding protein. Specific phosphorylation of Nephrin by a clustering strategy revealed that phosphorylation of Nephrin is directly involved in Ca^{2+} homeostasis via the recruitment and activation of PLC-γ1. Moreover, in a rat podocyte injury model, which is characterized by enhanced Nephrin phosphorylation, PLC-γ1 is phosphorylated and recruited to the plasma membrane. These results strongly suggest that the SD structure is directly linked to Ca^{2+} signaling by PLC-γ1 and demonstrate a novel role of SD as an orchestrator of a versatile signaling pathway, including Ca^{2+} homeostasis.

EXPERIMENTAL PROCEDURES

Antibodies and Reagents—Mouse monoclonal anti-FLAG antibody (M2; Sigma), rabbit polyclonal anti-PLC-γ1 antibody (Santa Cruz Biotechnology, Inc., Santa Cruz, CA), rabbit polyclonal anti-p-PLC-γ1 antibody (Tyr(P)-783) (Cell Signaling Technology, Danvers, MA), mouse monoclonal anti-phosphotyrosine antibody (4G10; Upstate Biotechnology, Inc., Lake Placid, NY), and mouse monoclonal anti-His antibody (Qiagen, Hilden, Germany) were obtained commercially. A rabbit polyclonal anti-Nephrin antibody was raised against a COOH-terminal peptide of 17 amino acids CAVEASSLPFELRGHLV (the first cysteine is not part of the Nephrin sequence) coupled to keyhole limpet hemocyanin. The antiserum was affinity-purified using the immunogen coupled to a SulfoLink column (Pierce). A rabbit polyclonal phosphospecific antibody (anti-Tyr(P)-1204) was raised against a high pressure liquid chromatography-purified synthetic oligopeptide CAWGPLpYDEVRMD. The antiserum was affinity-purified by the immunogen described above and absorbed with nonphosphorylated peptide, CAWGPLYDEVRMD. Western blotting was carried out with these antibodies diluted at 1:2000. Thapsigargin, U73122, and NAADP receptor modulator (catalog number 481919) were obtained from Calbiochem. NAADP receptor modulator is a weak NAADPR ligand (IC$_{50}$ = 90 μM in competition binding against 0.2 nM NAADP) that specifically inhibits NAADP-

mediated (but not cADPR-, inositol 1,4,5-trisphosphate (IP$_3$)-, or acetylcholine-evoked) Ca^{2+} response in sea urchin egg homogenate and in murine pancreatic acinar cells (17). 8-bromo-cyclic adenosine diphosphate ribose was from Sigma.

Cell Culture and Transfection—HEK293T cells were purchased from the ATCC (Manassas, VA). These cells were maintained in Dulbecco's modified Eagle's medium containing 10% fetal calf serum. NIH3T3 cells were cultured in Dulbecco's modified Eagle's medium containing 10% calf serum. Transfections were performed using Lipofectamine 2000 reagent (Invitrogen), following the manufacturer's instructions.

Eukaryotic Expression Constructs—The following plasmids were prepared. For full-length Nephrin and full-length Nephrin-FLAG, a cDNA fragment coding for full-length rat Nephrin was amplified by PCR using primers (5′-atttgcggccgcccgccatgggcgctaagagagtcactg-3′ and 5′-gcggtcgactcacaccagatgtcccctcagctc-3′, 5′-atttgcggccgcccgccatgggcgctaagagagtcactg-3′ and 5′-gcggtcgaccaccagatgtcccctcagctc-3′) and was cloned into a pCMV-Tag4A vector (Stratagene, Cedar Creek, TX). A Nephrin phenylalanine substitution mutant, Y1204F, was prepared using standard PCR methods. Mammalian expression plasmid encoding Fyn (18), FLAG-tagged PLC-γ1, and GFP-tagged PLC-γ1 (gift from P. G. Suh, POSTECH, Pohang, Korea) (19), and CD8 (gift from S. Yamasaki, RIKEN Research Center for Allergy and Immunology) (20) were as previously described. Restriction digestion and DNA sequencing were performed to validate all constructs.

Bacterial Fusion Protein Expression—A rat Nephrin cDNA fragment encoding the 151-amino acid cytoplasmic region (Nephrin-CD; amino acids 1102–1252) flanked with EcoRI (5′) and XhoI (3′) restriction sites was subcloned into pGEX-6P-1 (GE Healthcare). Bacterial pellets were resuspended and sonicated in a solution containing 20 mM Tris-HCl (pH 7.5), 150 mM NaCl, 1% Nonidet P-40, 2 mM dithiothreitol, 1 mM phenylmethylsulfonyl fluoride, 10 μg/ml antipain, and 10 μg/ml leupeptin; insoluble material was removed by centrifugation. GST-tagged fusion protein was purified on a glutathione-Sepharose column, followed by removal of GST with PreScission protease according to the manufacturer's instructions (GE Healthcare). To express the His-tagged NH$_2$-terminal SH2 domain of PLC-γ1 SH2, a PLC-γ1 cDNA fragment encoding the 108-amino acid residues (amino acids 550–657) flanked with EcoRI (5′) and NotI (3′) restriction sites was cloned into the pET28a (+) vector (Novagen, Madison, WI). To express the His-tagged COOH-terminal SH2 domain of PLC-γ1, a PLC-γ1 cDNA fragment encoding the 90 amino acid residues (amino acids 667–756) flanked with EcoRI (5′) and NotI (3′) restriction sites was cloned into the pET28a (+) vector. His-tagged fusion protein was purified by a nickel-Sepharose column according to the manufacturer's instructions (GE Healthcare).

In Vitro Phosphorylation and Peptide Mass Analysis—Phosphorylation of recombinant Nephrin-CD (residues 1102–1252) was performed by incubation of 6.0 μg of Nephrin-CD with 30 ng of recombinant active Fyn (Upstate Biotechnology) in 10 μl of kinase buffer (20 mM Tris-HCl, pH 7.5, 20 mM MgCl$_2$, 1 mM ATP, and 1 mM sodium orthovanadate) for 60 min at 30 °C. Phosphorylated Nephrin-CD was digested with trypsin (Promega, Madison, WI). Acetonitrile was added to a final concen-

tration of 90%, and the sample was desalted/concentrated using ZipTip HPL (Millipore, Bedford, MA). Peptides were eluted with 1 μl of matrix solution (0.1% acetic acid and 50% acetonitrile saturated with α-cyano-4-hydroxycinnamic acid) and applied onto a sample plate (Applied Biosystems, Foster City, CA). Matrix-assisted laser desorption ionization time-of-flight (MALDI-TOF) mass spectrometry was performed using Voyager-DE PRO (Applied Biosystems).

Pull-down Assay—GST or GST-Nephrin-CD immobilized on glutathione-Sepharose beads (GE Healthcare) was incubated with Fyn in a kinase buffer for 60 min at 30 °C. HEK293T cell lysates were incubated at 4 °C overnight with phosphorylated GST-Nephrin-CD or GST immobilized on beads. Beads were washed extensively with wash buffer (50 mM Tris-HCl, pH 7.5, 150 mM NaCl, 1% Nonidet P-40). Nephrin and bound proteins were detached from the beads by digestion with PreScission protease and analyzed by Western blotting or silver staining.

Determination of Proteins of Interest Using Mass Spectrometry—The pull-down sample prepared as above in large scale was subjected to SDS-PAGE and transferred to ProBlott membranes (Applied Biosystems) and stained with Coomassie Brilliant Blue. Proteins of interest were excised, treated with a reduction buffer (0.5 M Tris, pH 8.5, 8 M guanidine hydrochloride, 0.3% EDTA, 5% acetonitrile), and digested with 1 pmol of lysylendopeptidase (Wako) in 6 μl of digestion buffer (18 mM Tris, pH 8.9, 70% acetonitrile) for 90 min at 37 °C. Peptides were purified and subjected to peptide mass fingerprinting, as described above. Peptide ions specific for each sample were then used to interrogate human protein sequences in the NCBInr data base using the MASCOT algorithms.

Immunoprecipitation—Cells were lysed with immunoprecipitation buffer (20 mM Tris-HCl, pH 7.5, 150 mM NaCl, 1% Nonidet P-40, 1 mM phenylmethylsulfonyl fluoride, 10 μg/ml antipain, 10 μg/ml leupeptin, 100 units/ml aprotinin, 50 mM NaF, 1 mM EDTA, and 1 mM orthovanadate) for 15 min on ice. Lysates were clarified by centrifugation and incubated with beads conjugated with M2 anti-FLAG antibody for 1 h at 4 °C. Beads were washed twice with immunoprecipitation buffer, and bound proteins were eluted with 100 mM glycine-HCl (pH 2.6).

Immunohistochemistry—Immunofluorescence studies were performed as previously described (21). Briefly, rat kidneys were perfused with 2% paraformaldehyde fixative buffered with 0.1 M phosphate buffer (pH 7.4). These samples were immersed in the same fixative for about 30 min. After washing with phosphate-buffered saline (PBS), the tissue was immersed successively in PBS solution containing 10, 15, and 20% sucrose. After the tissue was embedded in OCT Compound and frozen, cryosections (thickness 5–10 μm) were cut using a Jung Frigocut 2800E (Leica) and then mounted on silane-coated glass slides. The cryosections were rinsed with PBS and blocked in blocking solution (0.1% bovine serum albumin in PBS). The sections were incubated with the primary antibodies and visualized with fluorescein isothiocyanate or rhodamine-isothiocyanate-conjugated second antibodies (Jackson ImmunoResearch Laboratories, West Grove, PA). Fluorescent specimens were viewed
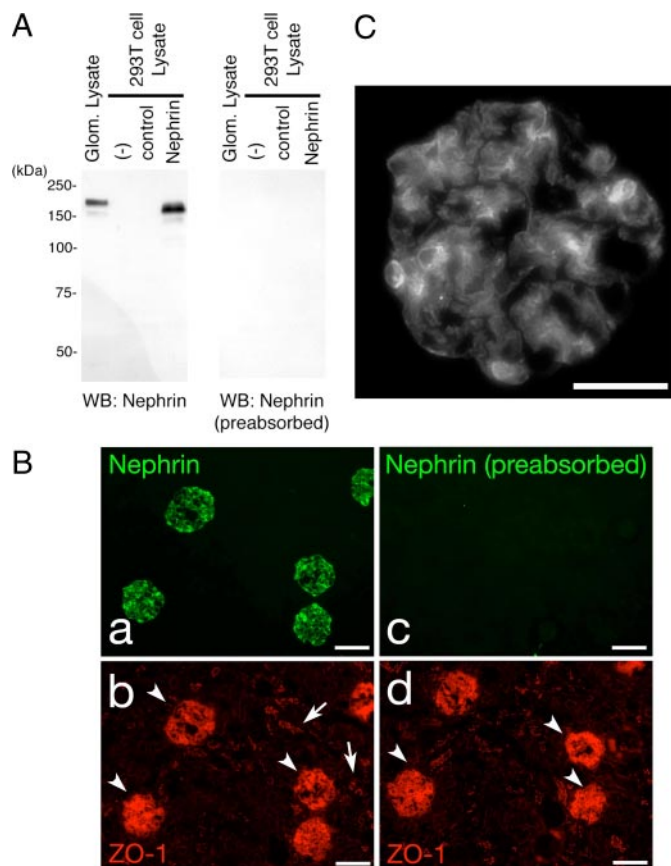

FIGURE 1. **Detection of Nephrin with the anti-Nephrin antibody.** *A*, lysates from isolated rat glomeruli, untransfected HEK293T cells, and HEK293T cells transiently transfected with plasmid encoding Nephrin or a control vector were separated on SDS-PAGE (10%), transferred to nitrocellulose membrane, and immunoblotted with anti-Nephrin (*left*) or anti-Nephrin preabsorbed with the peptide used for immunization (*right*). *B*, adult rat cryosections were analyzed by indirect immunofluorescence microscopy (magnification, ×100) after incubating sections simultaneously with anti-zonula occludens (*ZO-1*) and rabbit Nephrin antibody (*a* and *b*) or anti-Nephrin antibody preabsorbed with the peptide used for immunization (*c* and *d*) to confirm Nephrin staining in glomeruli (*arrowheads*) but not in the tubular cells (*arrows*). *Scale bars*, 100 μm. *C*, nephrin staining shows a typical podocyte pattern along the glomerular capillary loops. Magnification, ×400; *scale bars*, 50 μm.

with a confocal laser-scanning microscope LSM510 (Carl Zeiss, Thornwood, NY).

Immunoelectron Microscopy—Kidneys were isolated from anesthetized adult rats, which were fixed by perfusion of 0.5% (w/v) glutaraldehyde in PBS. Tissues were cut in small pieces and fixed in the same fixative for 1 h on ice, washed with PBS, and dehydrated with a graded series of ethanol. Cubes of renal cortex (2 mm) were embedded in LR white resin (London Resin Company Ltd., London, UK) and polymerized with LR white accelerator and stored at −20 °C. Ultrathin sections were mounted on 300-mesh nickel grids and treated with 3% H_2O_2 for 10 min. After blocking with 1% (w/v) bovine serum albumin in PBS for 30 min, grids were incubated overnight at 4 °C with the affinity-purified rabbit anti-PLC-γ1 antibody, washed with PBS, and incubated with 10-nm gold-conjugated goat anti-rabbit IgG (GE Healthcare) at a dilution of 1:20 for 1 h at room temperature. Grids were washed with distilled water and stained with uranyl acetate for 20 min. After air drying at room temperature, the sections were photographed on a Hitachi 7100 electron microscope at ×10,000 magnification.
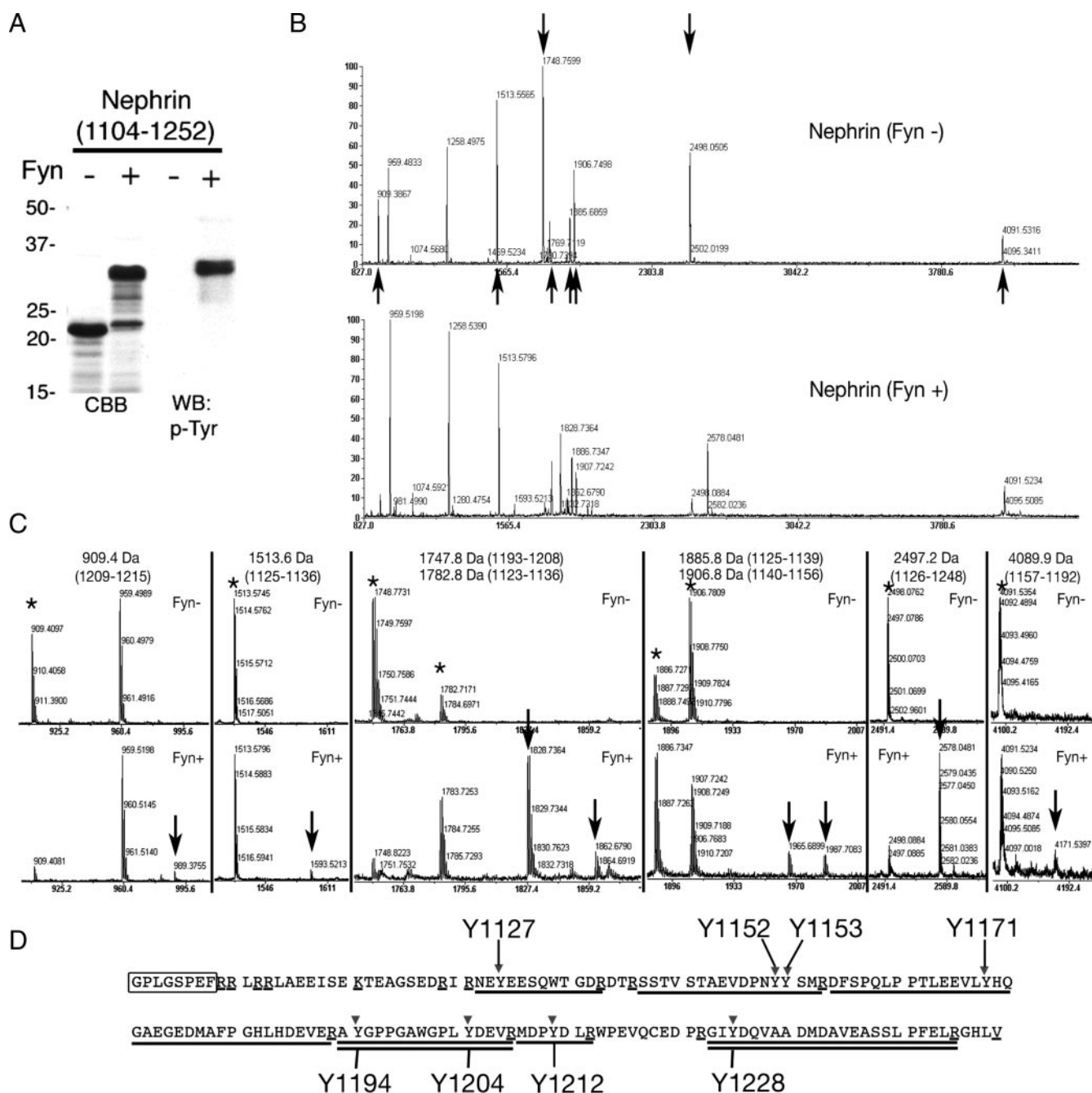
FIGURE 2. **Tyrosine phosphorylation of Nephrin by Fyn *in vitro*.** *A*, Nephrin-CD (amino acids 1104–1252) was incubated with or without Fyn *in vitro*, and the samples were immunoblotted with anti-phosphotyrosine (*p-Tyr*) antibody. *CBB*, Coomassie Brilliant Blue staining; *WB*, Western blot. *B*, identification of tyrosine residues of Nephrin phosphorylated by Fyn. The same samples as in *A* were digested with trypsin, and the peptides were analyzed by a MALDI-TOF mass spectrometer. A marked decrease of peak intensity was observed for two peptides (indicated by *downward arrows*; 1747.8 Da (corresponding to amino acids 1193–1208) and 2497.2 Da (residues 1226–1248)), and a moderate decrease was observed for other peptides (909.4 Da (residues 1209–1215), 1513.6 Da (residues 1125–1136), 1782.8 (residues 1123–1136), 1885.8 (residues 1125–1139), 1906.8 Da (residues 1140–1156), and 4089.9 Da (residues 1157–1192); *upward arrows*). Representative data are shown from one of three independent experiments. *C*, detailed data of the peptide mass spectra of nonphosphorylated (*top*) and phosphorylated (*bottom*) Nephrin-CD in Fig. 2*B* are shown. *D*, tyrosine phosphorylation sites in the rat Nephrin-CD. The amino acid sequence of Nephrin-CD with amino-terminal linker sequence (the first eight amino acids, marked as a *box*). Peptides corresponding to 1747.8 and 2947.2 Da are *double underlined*. Peptides corresponding to 909.4 Da (residues 1209–1215), 1513.6 Da (residues 1125–1136), 1906.8 Da (residues 1140–1156), and 4089.9 Da (residues 1157–1192) are *underlined*. Candidate phosphorylation sites are indicated by *arrows* with *amino acid numbers*. Lysine and arginine residues are marked with *single underlines*.

CD8 Chimera Clustering—NIH 3T3 cells were transfected with CD8 chimeric constructs bearing Nephrin-CD at the COOH-terminal end. At 24 h after transfection, Dulbecco's modified Eagle's medium was removed and replaced with fresh medium containing 1 μg/ml CD8 antibody (clone RPA-T8, BD Biosciences). Cells were maintained at 37 °C for 10 min. At this point, cells were washed with PBS and replaced with medium containing 1 μg/ml goat anti-mouse IgG (Pierce), and incubation was continued for 15 min for the recruitment experiment. Cells were washed three times with PBS and fixed with 3.7%

formaldehyde for 10 min at room temperature. Fixed cells were then permeabilized with 0.1% Triton X-100 for 10 min. After washing with PBS, the cells were incubated with primary antibodies in PBS containing 1% bovine serum albumin for 1 h, followed by incubation with Alexa Fluor-conjugated secondary antibodies (1:1000 dilution; Invitrogen) for 1 h. Coverslips were mounted on glass slides using ProLong Gold antifade reagent (Invitrogen Corp.). Samples were observed on an inverted microscope (model IX71; Olympus, Tokyo, Japan) equipped with a PlanApo ×60, 1.4 numerical aperture oil immersion objective. Images were obtained with a cooled charge-coupled device camera (ORCA-ER; Hamamatsu Photonics, Shizuoka, Japan) controlled by Aqua-Lite software (Hamamatsu Photonics) and were processed using Adobe Photoshop CS3.

Inositol 1,4,5-Trisphosphate Generation Assay—HEK293T cells (2.4×10^6) were transfected with CD8/Nephrin-CD and PLC-γ1 vectors. These cells were stimulated with the primary antibody for 10 min at 37 °C and the secondary antibody for the indicated times at 37 °C. Determination of IP_3 production was performed using the Biotrak IP_3 assay system (GE Healthcare) according to the manufacturer's protocol. Ratios compared with the control (secondary antibody: 0 min) are shown as the mean of three independent experiments. *Error bars* represent the S.D.

Determination of $[Ca^{2+}]_i$ Changes with the Ratiometric Pericam—The intracellular Ca^{2+} change was measured using a fluorescent Ca^{2+} indicator, ratiometric pericam (22). HEK293T cells expressing the ratiometric pericam were analyzed by video imaging using a multidimensional imaging work station (AS MDW, Leica Microsystems, Wetzlar, Germany) with dual alternative excitations at 410 and 490 nm and detection with a fluorescent emission filter, 520–600 nm. The 490 nm/410 nm excitation ratio, which increases as a function of intracellular Ca^{2+}, was captured at 5-s intervals.

Animals—All the experiments using model animal were carried out according to the guidelines set by the Animal Center of the Institute of Medical Science at the University of Tokyo. Perfusion of rat kidneys with protamine sulfate (PS) was carried out essentially as previously described (21). Six-week-old male Wistar rats were purchased from Charles River Laboratories Japan, Inc. (Atsugi, Japan). The rats were anesthetized with pentobarbital. Kidneys were perfused through the aorta at 5 ml/min with Hanks' balanced salt solution for 20 min followed by PS solution (500 μg/ml in Hanks' balanced salt solution) for 20 min. The cryostat sections for immunohistological study and glomerular lysates were prepared as previously described (23).

RESULTS

Characterization of Anti-Nephrin Antibody—We prepared a rabbit polyclonal antibody against the rat Nephrin carboxyl-terminal 17 amino acid residues. To assess the specificity of the antibody, the full-length rat Nephrin cDNA was cloned and transiently expressed in human embryonic kidney HEK293T cells. A portion of the cell lysates was subjected to immunoblotting with this antibody. As shown in Fig. 1A, the anti-Nephrin antibody recognized a protein with an apparent molecular mass of ~180 kDa in the Nephrin-transfected cells but not in the
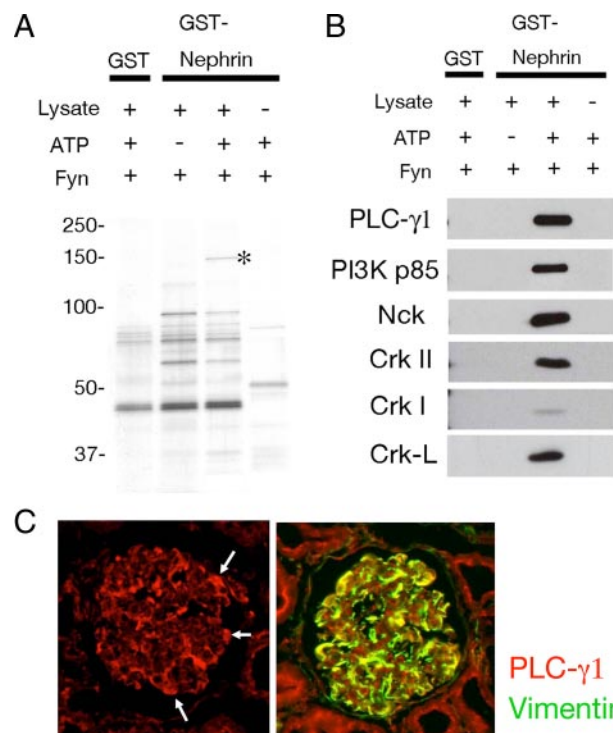

FIGURE 3. **Identification of PLC-γ1 as a phospho-Nephrin-binding protein.** *A*, recombinant GST-Nephrin-CD was bound to glutathione-Sepharose beads and incubated with recombinant Fyn with or without ATP. After washing, the beads were incubated with lysates from HEK293T cells, and bound proteins were analyzed by silver staining. These experiments were repeated four times, and representative data are shown. *B*, multiple proteins specifically bind to phosphorylated Nephrin. Protein samples in *A* were analyzed by immunoblotting for the indicated antibodies. *C*, expression of PLC-γ1 in podocytes. Indirect immunofluorescence microscopy was performed to detect PLC-γ1 in adult rat kidney cryosections (*left*). Colocalization with vimentin suggests that PLC-γ1 is highly expressed in podocyte in renal glomeruli (*right*). Magnification was ×400.

empty vector transfectants. Rat glomeruli were isolated using a sieving protocol (21), and their extracts were analyzed similarly. A protein with a slightly slower mobility than overexpressed Nephrin in HEK293T cells, probably due to a difference in post-translational modification, was clearly visible. We immunostained kidney sections isolated from normal rats with this antibody, which resulted in a specific staining in renal glomeruli (Fig. 1B). Nephrin staining shows a typical podocyte pattern along glomerular capillary loops (Fig. 1C).

Identification of Tyrosine Residues of Nephrin Phosphorylated by Fyn—Recent studies have revealed that the SD protein complex conducts phosphorylation-mediated signals to integrate the junctional structure and cytoskeletal dynamics in podocytes. Nephrin is tyrosine-phosphorylated by Fyn in developing glomeruli and injured podocytes, recruiting Nck to the SD to regulate actin filament polymerization (12, 13). To extend our knowledge of the mechanism regulated by Nephrin phosphorylation, we first determined the tyrosine residues phosphorylated by Fyn. To identify these sites, we performed *in vitro* phosphorylation of Nephrin by recombinant active Fyn and confirmed that Nephrin-CD (cytoplasmic domain, amino acids 1104–1252) was tyrosine-phosphorylated by Fyn *in vitro* (Fig. 2A). The significant mobility shift indicates multiple phosphorylation and conformational changes of Nephrin-CD.
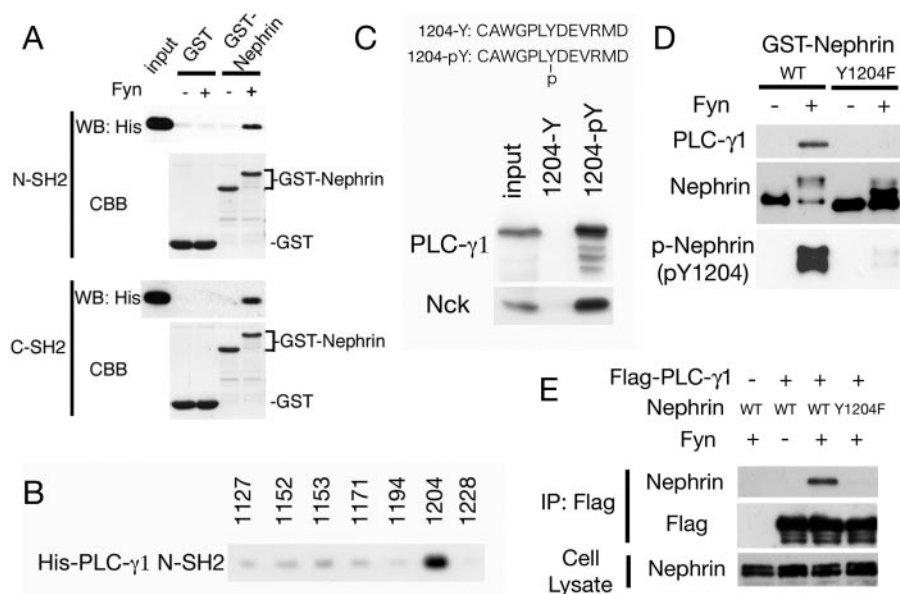
FIGURE 4. **PLC-γ1 directly binds to phosphorylated Nephrin Tyr(P)-1204.** *A*, recombinant GST or GST-Nephrin-CD was bound to glutathione-Sepharose beads and incubated with or without Fyn. After washing, the beads were incubated with recombinant His-tagged N- or C-SH2 domain of PLC-γ1, and bound proteins were immunoblotted with anti-His antibody. *CBB*, Coomassie Brilliant Blue staining. *WB*, Western blot. *B*, phosphorylated Nephrin peptides were immobilized to SulfoLink coupling gel to pull down His-PLC-γ1-N-SH2. PLC-γ1-N-SH2 specifically bound to phospho-Tyr-1204. *C*, phosphorylated or nonphosphorylated Nephrin Tyr-1204 peptides were immobilized to coupling gel and incubated with HEK293T cell lysates. The bound proteins were immunoblotted with anti-PLC-γ1 and anti-Nck. *D*, GST-Nephrin-CD wild type or Y1204F were phosphorylated by Fyn and immobilized to glutathione-Sepharose. The beads were incubated with HEK293T lysates, and bound proteins were analyzed by Western blotting for PLC-γ1. *E*, HEK293T cells were transfected with indicated vectors, and anti-FLAG immunoprecipitates (*IP*) and cell lysates were analyzed by Western blotting for FLAG and Nephrin.

HEK293T cells. Proteins trapped on the beads were analyzed by silver staining. As shown in Fig. 3*A*, a 150-kDa protein specifically bound to phosphorylated Nephrin (marked by an *asterisk*). This band was excised and subjected to peptide mass fingerprinting, as described under "Experimental Procedures." Using the MASCOT (available on the World Wide Web) data base search algorithms, this protein was identified as human PLC-γ1 (probability 9.8E-009, score 113, coverage 14%). Proteins trapped on the beads were also analyzed by immunoblotting using antibodies against several SH2 domain-containing proteins. Of these, Crk family proteins (CrkI, CrkII, and Crk-L), Nck, and phosphatidylinositol 3-kinase p85 also specifically bound to Nephrin in a phosphorylation-dependent manner (Fig. 3*B*). Rat glomerular cryosections were immunostained with antibody to PLC-γ1 (Fig. 3*C*, *left*). Although not restricted to podocytes, PLC-γ1 is highly expressed in podocytes, which are indicated by expression of the podocyte marker vimentin (Fig. 3*C*, *right*).

PLC-γ1 Directly Binds to Phosphorylated Tyr-1204 of Nephrin—Next, the interaction between Nephrin and PLC-γ1 was investigated. PLC-γ1 has two SH2 domains (N-SH2 and C-SH2). GST or GST-Nephrin-CD immobilized on glutathione beads phosphorylated by Fyn *in vitro* was incubated with either of the His-tagged SH2 domains of PLC-γ1, and bound proteins were analyzed by SDS-PAGE and immunoblotted with anti-His antibody. As shown in Fig. 4*A*, both SH2 domains directly bound to phosphorylated Nephrin. To identify the critical tyrosine residue for the interaction, pull-down analysis using phosphorylated Nephrin peptides was performed. Tyr-1212 was omitted, because this tyrosine is not conserved in human Nephrin. As shown in Fig. 4*B*, the PLC-γ1 N-SH2 domain specifically bound to phosphorylated Tyr-1204 peptide. The PLC-γ1 C-SH2 domain did not show specific binding to these peptides (data not shown). C-SH2 may be involved in intramolecular binding to Tyr-783, as described (24). Phosphorylation specificity was also examined by pull-down analysis using nonphosphorylated and phosphorylated Nephrin peptide around Tyr-1204. When the peptide-immobilized beads were incubated with HEK293T lysates, Nck and PLC-γ1 specifically bound to phosphorylated Tyr-1204 (Fig. 4*C*). Site specificity was also confirmed by pull-down analysis using GST-Nephrin Y1204F (Fig. 4*D*). We also confirmed this interaction in transiently transfected HEK293T cells. PLC-γ1 was specifically coimmunoprecipitated with Fyn-phosphorylated wild type Nephrin but not with nonphosphorylated Nephrin or with the phosphoryl-

These samples (phosphorylated and nonphosphorylated Nephrin-CD) were digested with trypsin, and their peptide mass fingerprints were compared. Fig. 2*B* shows the peptide mass spectra of nonphosphorylated (*top*) and phosphorylated (*bottom*) Nephrin-CD. When a peptide is phosphorylated, its peptide mass should increase by 80 Da. By this criterion, we could identify phosphorylated peptides by comparing these two spectra. In the Fyn-phosphorylated samples, significant decreases in peak intensity were observed for peptides of 1747.8 Da (corresponding to amino acids 1193–1208) and 2497.2 Da (amino acids 1226–1248) (indicated by *downward arrows* in Fig. 2*B*), and concomitantly phosphorylated forms of these peptides were identified. Similarly, partial phosphorylation of peptides of 909.4 Da (amino acids 1209–1215), 1513.6 Da (amino acids 1125–1136), 1782.8 (amino acids 1123–1136), 1885.8 (amino acids 1125–1139), 1906.8 Da (amino acids 1140–1156), and 4089.9 Da (amino acids 1157–1192) (Fig. 2, *B* (indicated by *upward arrows*) and *C*) were also observed. These results suggested that all of the eight tyrosine residues in rat Nephrin-CD can at least be partially phosphorylated *in vitro*, and of those, Tyr-1194, Tyr-1204, and Tyr-1228 are the major sites for the tyrosine phosphorylation.

Identification of SH2 Domain-containing Proteins That Associate with Phosphorylated Nephrin—To characterize the diverse function of Nephrin tyrosine phosphorylation, we investigated phospho-Nephrin-binding proteins by pull-down strategy. GST or GST-Nephrin-CD was immobilized on glutathione-Sepharose beads and phosphorylated by Fyn *in vitro*. These samples were used to pull down binding proteins from
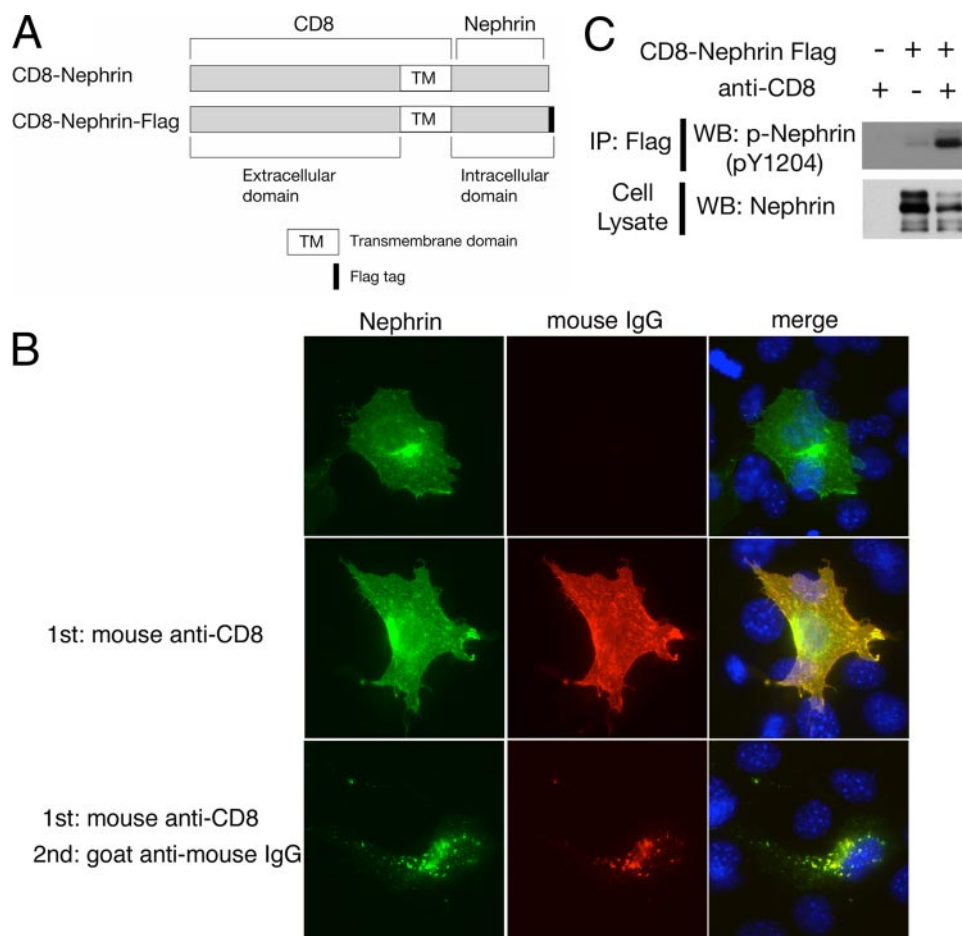
FIGURE 5. **Clustering of Nephrin-CD.** *A*, schematic representation of CD8 fusion proteins. *B*, clustering of the CD8/Nephrin-CD by cross-linking. HEK293T cells expressing CD8/Nephrin-CD were treated with mouse anti-CD8 (*middle panels*) or with anti-CD8 plus goat anti-mouse IgG (*lower panels*) and then fixed. Cells were stained with anti-Nephrin antibody (*green*), anti-mouse IgG antibody (*red*), and 4′,6-diamidino-2-phenylindole (*blue*). Representative data are shown. Magnification was ×100. *C*, HEK293T cells expressing CD8/Nephrin-CD-FLAG were treated with clustering antibodies (*left* and *right lanes*; primary + secondary antibody; *middle lane*; secondary antibody only), and then the cell lysates and FLAG immunoprecipitates (*IP*) were immunoblotted for Nephrin and phospho-Nephrin (Tyr(P)-1204). *WB*, Western blot.

extracellular domain and the transmembrane domain (amino acids 1–206) were coupled to Nephrin-CD (CD8/Nephrin-CD) (Fig. 5*A*). This fusion protein was expressed in cultured cells by transient transfection. After 24 h, a mouse anti-CD8 antibody and a secondary anti-mouse IgG antibody were added to the culture media. This procedure induced visible aggregation or clustering of the CD8 fusion protein on the plasma membrane (Figs. 5*B* and 6) and induced tyrosine phosphorylation on Tyr-1204 of CD8/Nephrin-CD (Fig. 5*C*). To test whether Nephrin clustering induces PLC-γ1 relocalization, NIH 3T3 cells were cotransfected with plasmids encoding CD8/Nephrin-CD and PLC-γ1-GFP and were examined by immunofluorescence. Upon clustering, a significant portion of PLC-γ1-GFP forms a dotlike structure, which colocalized with Nephrin-CD at the plasma membrane, as stained by anti-CD8 (Fig. 6). Approximately 60–70% of CD8-Nephrin clusters contain PLC-γ1. We did not detect any PLC-γ1 clusters where anti-CD8 antibody was not present. These results clearly indicate that Nephrin clustering recruits PLC-γ1 to Nephrin-CD.

Clustering of Nephrin Activates PLC-γ1 and Induces Ca²⁺ Response—

ated Y1204F mutant (Fig. 4*E*). These results indicate that PLC-γ1 directly binds to phosphorylated Tyr-1204 of Nephrin.

*Nephrin Clustering Induces Its Phosphorylation and Recruits PLC-γ1 to Nephrin-CD—*The phosphorylated tyrosine residues in receptors for growth factors, immunoglobulins, and cytokines provide a set of specific docking platforms to recruit various effector proteins, including PLC-γ. The recruitment of PLC-γ to tyrosine-phosphorylated growth factor receptors activates PLC-γ and mobilizes the internal Ca²⁺ stores and further affects multiple downstream protein kinase pathways that control or modulate diverse cellular functions. It is already known that upon clustering of Nephrin-CD, the Src family protein kinase rapidly catalyzes the phosphorylation of Nephrin. Phosphorylated Nephrin recruits Nck to the plasma membrane, which results in concomitant recruitment of components of the actin polymerization complex and induction of localized actin polymerization (12, 13). We sought to test the hypothesis that in a similar fashion, PLC-γ1 may be recruited to Nephrin-CD at the plasma membrane. To this end, a modified strategy developed by Verma *et al.* (12) and Jones *et al.* (13) was used. A fusion protein construct was created in which the CD8

Recruitment of PLC-γ to growth factor receptors results in its tyrosine phosphorylation, and this phosphorylation is necessary for its activation. Although PLC-γ1 is rapidly phosphorylated at Tyr-771 and Tyr-783 in response to epidermal growth factor and platelet-derived growth factor receptor kinases, Tyr-783 is known to be crucial for the activation of PLC-γ1 through its intramolecular interaction with C-SH2 (24). Therefore, we examined whether PLC-γ1 is phosphorylated and activated in response to Nephrin phosphorylation using phosphospecific antibody for PLC-γ1 Tyr(P)-783. When HEK293T cells expressing FLAG-tagged CD8/Nephrin-CD and FLAG-tagged PLC-γ1 were treated with the primary and secondary antibodies, clustering-induced tyrosine phosphorylation of Nephrin on Tyr-1204 occurred within 1 min of the addition of clustering antibodies, and Tyr(P)-1204 was quickly dephosphorylated after 4–5 min (Fig. 7*A*). On the other hand, phosphorylation of PLC-γ1 Tyr-783 was observed 2 min after antibody treatment and persisted for more than 45 min (Fig. 7, *A* and *B*). The phosphorylation of PLC-γ1 Tyr-783 was absolutely dependent on Nephrin Tyr-1204 phosphorylation, because Y1204F mutant did not induce this phosphorylation at all (Fig. 7*C*).
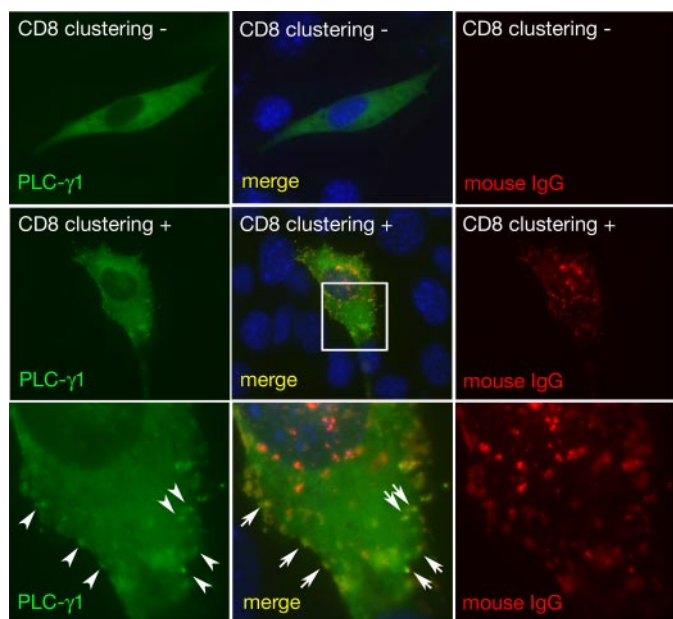
FIGURE 6. PLC-γ1 is recruited to the CD8/Nephrin-CD cluster. NIH3T3 cells expressing CD8/Nephrin-CD and PLC-γ1-GFP (*green*) were treated with mouse anti-CD8 antibody and goat anti-mouse IgG antibody (*middle* and *lower panels*) or were treated with the secondary antibody only (*upper panels*) and then fixed and stained for mouse IgG (*red*) and 4′,6-diamidino-2-phenylindole (*blue*). Higher magnification images corresponding to a *square* in a *middle panel* are shown in the *lower panels*. PLC-γ1 forms clusters upon CD8 clustering and the clusters were colocalized with CD8/Nephrin-CD clusters. Magnification was ×400.

The activation of PLC-γ induced by stimulation of surface membrane receptors triggers hydrolysis of phosphatidylinositol 4,5-bisphosphate into IP_3 and diacylglycerol and elicits Ca^{2+} signals. Therefore, we measured IP_3 levels in cells treated with clustering antibodies. As shown in Fig. 7*D*, clustering of Nephrin-CD resulted in generation of IP_3 within 2 min, which is well correlated with the activation of PLC-γ1.

We next examined whether this clustering-induced activation of PLC-γ1 is involved in Ca^{2+} signaling. HEK293T cells were cotransfected with CD8/Nephrin-CD and PLC-γ1. Real time changes in the cytosolic free Ca^{2+} concentration ($[Ca^{2+}]_i$) were monitored in individual cells, using the Ca^{2+}-selective sensor pericam (22). The fluorescence ratio at 490 nm excitation to that of 410 nm excitation reflects $[Ca^{2+}]_i$ at a constant pH (22). Clustering of Nephrin-CD triggered a rapid rise in pericam excitation ratio 490 nm/410 nm (Fig. 8*A*), indicating a clustering-induced $[Ca^{2+}]_i$ rise. Both CD8/Nephrin-CD and PLC-γ1 were necessary for this clustering-induced $[Ca^{2+}]_i$ change, because the omission of either component abolished the Ca^{2+} response (Fig. 8, *B* and *C*). No increase in $[Ca^{2+}]_i$ was observed when HEK293T cells cotransfected with CD8/Nephrin-CD and PLC-γ1 were treated with either the first or second antibody alone (Fig. 8, *D* and *E*), demonstrating the specificity of the clustering response. Because no change in $[Ca^{2+}]_i$ was observed when cells expressing CD8/Nephrin-CD Y1204F mutant, which does not bind to PLC-γ1, were treated with clustering antibodies (Fig. 8*F*), the recruitment of PLC-γ1 to Nephrin Tyr-1204 is crucial for the Ca^{2+} signal. To examine whether the rise in $[Ca^{2+}]_i$ in response to Nephrin clustering originated primarily from internal Ca^{2+} store release or external Ca^{2+} influx, HEK293T cells transfected with CD8/Nephrin-CD and PLC-γ1 were stimulated with clustering antibodies in the absence of extracellular Ca^{2+} (Fig. 8*G*). The initial transient rise in $[Ca^{2+}]_i$ of clustering-stimulated cells was still observed under these conditions, suggesting that at least some of the Ca^{2+} response originates from internal stores. When the cells were pretreated with thapsigargin (a SERCA pump inhibitor) to deplete internal Ca^{2+} stores (Fig. 8*H*), there was no Ca^{2+} response in cells treated with clustering antibodies. Furthermore, a PLC inhibitor, U73122, partially inhibited the sustained increase in $[Ca^{2+}]_i$, suggesting the involvement of PLC-γ1 activity in the Ca^{2+} response (Fig. 8*I*). Recently, other Ca^{2+}-mobilizing messengers, such as cADP-ribose and NAADP (nicotinic acid-adenine dinucleotide phosphate), have been shown to be involved in
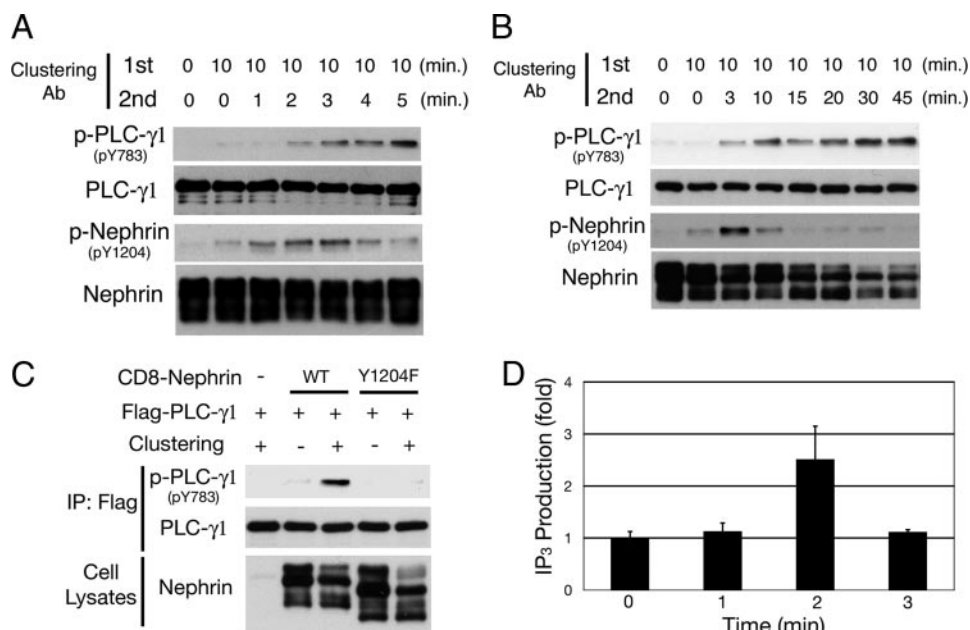

FIGURE 7. Nephrin clustering activates PLC-γ1. *A* and *B*, HEK293T cells expressing FLAG-tagged PLC-γ1 and CD8/Nephrin-CD were treated with or without mouse anti-CD8 antibody for 10 min and then with goat anti-mouse IgG antibody for the indicated periods of time. Anti-FLAG immunoprecipitates were analyzed by Western blotting with the antibodies indicated. Nephrin is phosphorylated in 1 min after CD8/Nephrin-CD clustering and dephosphorylated after 4–5 min, whereas phosphorylation of PLC-γ1 is observed after 2 min and continues for over 45 min. *C*, phosphorylation of PLC-γ1 is abrogated by substitution of Tyr-1204 to Phe, indicating the critical role of this tyrosine in the activation of PLC-γ1. Incubation time for the secondary antibody was 15 min. *IP*, immunoprecipitation; *WT*, wild type. *D*, IP_3 production. IP_3 levels in these cells were measured using a competitive binding assay with radiolabeled IP_3-binding proteins. Three independent competitive radioreceptor assays for IP_3 levels in the cells as in *A* were performed, and the mean values are shown with S.D.
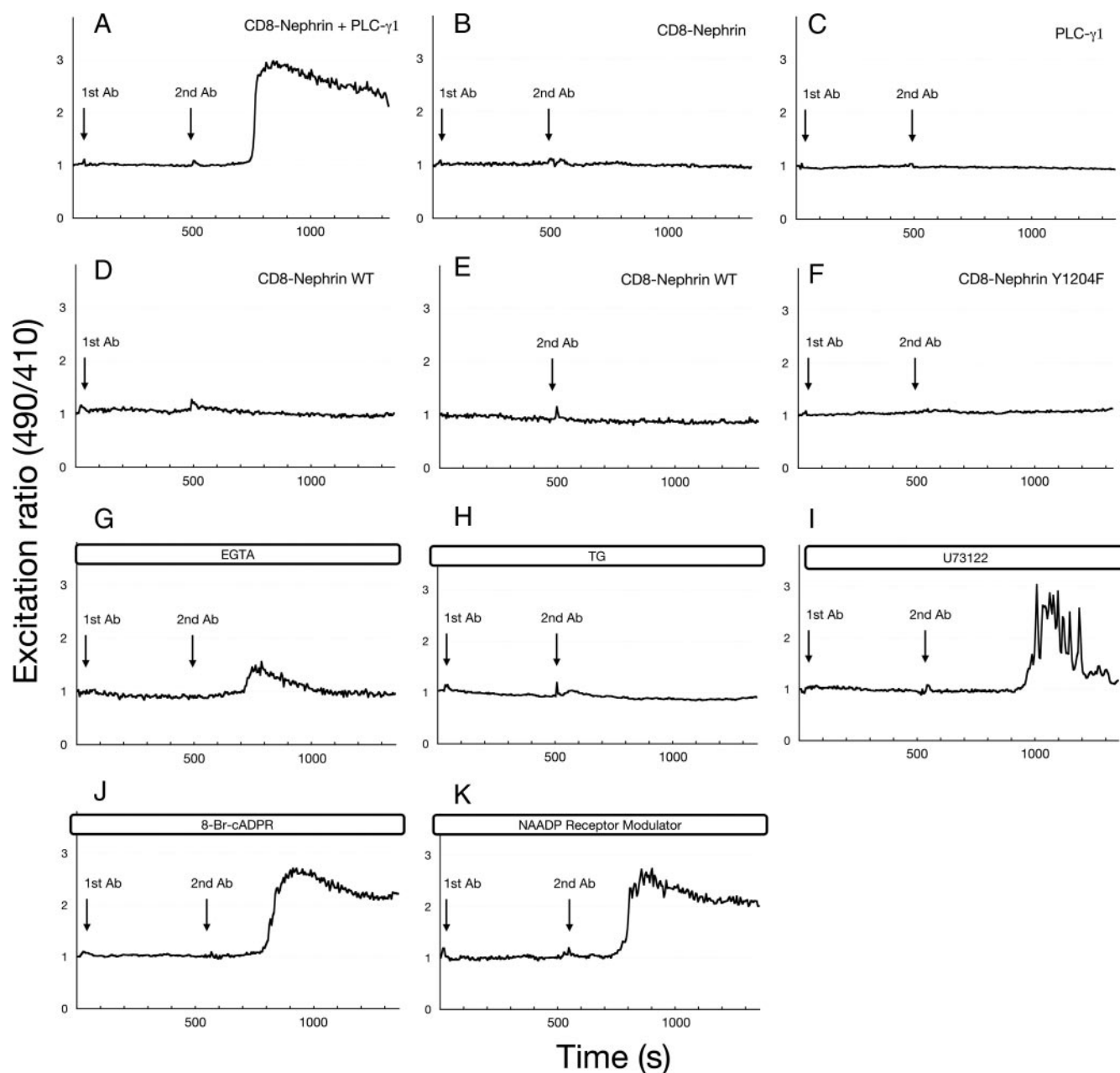
FIGURE 8. **Nephrin clustering triggers Ca²⁺ response.** The Ca²⁺ concentration was monitored in HEK293T cells transiently expressing a fluorescent protein, pericam, whose fluorescence spectral properties change reversibly upon Ca²⁺ binding. The 490 nm/410 nm excitation ratios of pericam are plotted against the elapsed time. *A*, representative time course of the Ca²⁺ response upon CD8/Nephrin-CD clustering in cells expressing both CD8/Nephrin-CD and PLC-γ1. *B* and *C*, the Ca²⁺ response was not observed in cells expressing either CD8/Nephrin-CD or PLC-γ1. *D* and *E*, [Ca²⁺]$_i$ rise was not observed when cells expressing CD8/Nephrin-CD and PLC-γ1 were treated with either the primary or secondary clustering antibody alone. *F*, cells expressing CD8/Nephrin-CD Y1204F and PLC-γ1 did not respond to CD8 clustering. *G*, initial transient rise of [Ca²⁺]$_i$ was observed in the absence of extracellular Ca²⁺ (EGTA). *H*, HEK293T cells pretreated with thapsigargin (a SERCA pump inhibitor) (2 μM) did not respond to clustering treatment. *I*, a PLC inhibitor, U73122 (20 μM), partially abrogated the Ca²⁺ response. *J*, antagonistic cADPR did not block the Ca²⁺ response. The concentration of 8-Br-cADPR was 100 μM. *K*, NAADP receptor modulator (1 mM) did not affect the response. Each experiment was performed at least five times, and representative data are shown.

cellular Ca²⁺ homeostasis (25, 26); however, they do not seem to contribute to the clustering-induced [Ca²⁺]$_i$ rise, because their inhibitors did not block this Ca²⁺ response (Fig. 8, *J* and *K*).

Phosphorylation of Nephrin and PLC-γ1 in Injured Podocytes in Vivo—Previous studies have demonstrated that several SD components are tyrosine phosphorylated in the PS-induced podocyte injury model (12, 21, 27, 28). To understand the role of Nephrin-PLC-γ1 signaling in the kidney *in vivo*, we tested

whether treatment with PS induces the activation of PLC-γ1. PLC-γ1 was immunoprecipitated with anti-PLC-γ1 antibody from glomerular lysates of normal or PS-treated rats, and the immunoprecipitates were immunoblotted with anti-PLC-γ1 or anti-phospho-PLC-γ1 (Tyr(P)-783). As shown in Fig. 9*B*, PLC-γ1 Tyr-783 was significantly phosphorylated in PS-treated glomeruli. Nephrin Tyr-1204, the binding site for PLC-γ1, was also phosphorylated to a significant level (Fig. 9*A*). Electron microscopy of immunogold-labeled ultrathin cryosec-
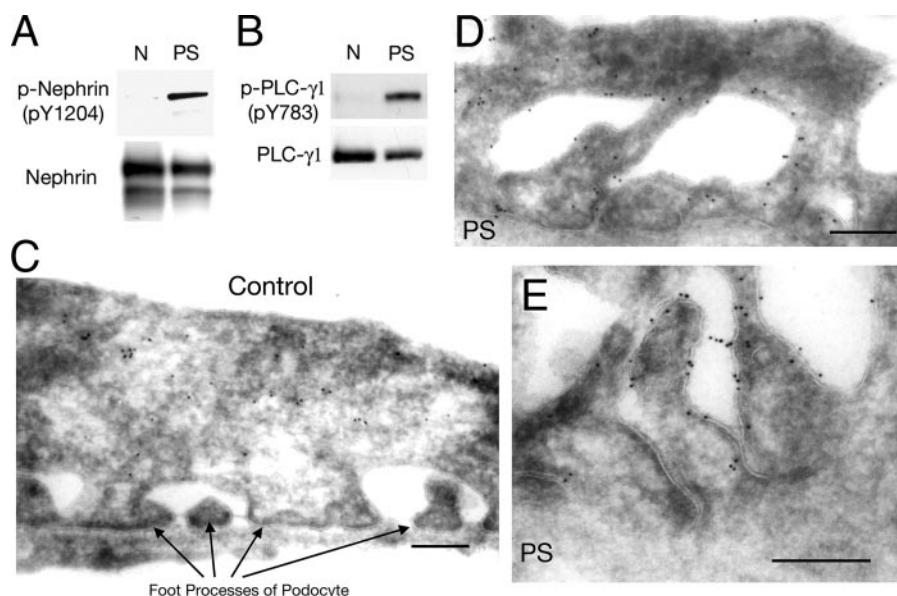
FIGURE 9. **PLC-γ1 is phosphorylated in injured podocytes** *in vivo.* *A* and *B*, rat kidneys were perfused with protamine sulfate (*PS*) or control solution (*N*) as described under "Experimental Procedures." Glomerular lysates were immunoprecipitated by anti-Nephrin antibody and anti-PLC-γ1 antibody, and the immunoprecipitates were resolved by SDS-PAGE and immunoblotted with the indicated antibodies. *C–E*, altered localization of PLC-γ1 in podocytes in the PS model. Kidney sections from normal rats (*C*) or PS-treated rats (*D* and *E*) were analyzed by immunoelectron microscopy after incubating sections with anti-PLC-γ1 antibody and 10-nm gold-conjugated secondary antibody. Representative data are shown from one of three independent experiments. *Scale bars*, 0.2 μm.

both Nephrin and PLC-γ1 are also found to be phosphorylated in an *in vivo* podocyte injury model.

Ca^{2+} is a universal cellular messenger and is precisely controlled in all cell types. The dynamic changes in its release from the endoplasmic reticulum and its entry from the extracellular space trigger a plethora of cellular responses. Central to this schema are members of the PLC superfamily, which relay information from the activated receptors to downstream signal cascades by production of second messenger molecules, IP_3 and diacylglycerol. In our system, Nephrin clustering induces phosphorylation of PLC-γ1 and triggers a rapid $[Ca^{2+}]_i$ rise. Both PLC-γ1 phosphorylation and Ca^{2+} mobilization are dependent on the phosphorylation of Nephrin Tyr-1204, the binding site for PLC-γ1. This Ca^{2+} mobilization requires internal Ca^{2+} store release, because thapsigargin, which depletes calcium stores, completely abrogated the clustering-induced Ca^{2+} mobilization. Ca^{2+} entry from the ion channels on the plasma membrane contributes to the persistent $[Ca^{2+}]_i$ rise, because only the initial transient rise in $[Ca^{2+}]_i$ was observed when extracellular calcium was depleted by EGTA. In the presence of a PLC inhibitor, U73122, the persistent $[Ca^{2+}]_i$ rise was partially abrogated, suggesting that PLC-γ1 activity is required for this phase. In relevance to this partial inhibition, it is of note that previous studies have led to the suggestion that the PLC-γ can function as a molecular component of agonist-initiated Ca^{2+} entry mechanisms, independent of its catalytic activity (37–39). PLC-γ possesses several protein-protein interaction domains that interact with transient receptor potential channels (37, 38) and seemingly promotes Ca^{2+} entry (40). It is also known that U73122 inhibits the activation of the Ca^{2+} release-activated Ca^{2+} channel and that this role of PLC is unrelated to IP_3 and to IP_3 receptors (41). Although it is difficult to clearly define the Ca^{2+} entry channels and the molecular mechanisms involved in our clustering system, in light of these previous results, our results suggest that PLC-γ1 may in part trigger the Ca^{2+} entry pathway independently of its catalytic activity.

In the clustering system used in the present study, Nephrin clustering induces phosphorylation of PLC-γ1 and rise of IP_3 concentration within 2 min and triggers a $[Ca^{2+}]_i$ rise after various periods of time (231.9 ± 54.1 s from the addition of the secondary antibody). The variety in the time intervals between the addition of secondary antibody and the $[Ca^{2+}]_i$ rise may be explained by the difference in the expression levels of CD8/Nephrin-CD or PLC-γ1 in each cell that modulate the signal intensity and durability. In fact, there was a strong tendency for longer intervals in the U73122-treated cells (441.3 ± 139.6 s). Stimulus-induced Ca^{2+} responses are thought to be formed by

tions revealed that PLC-γ1 was localized mainly in the cytoplasm in normal podocytes (Fig. 9*C*), whereas the signals of PLC-γ1 in injured podocytes were mainly observed on the plasma membrane of the effaced podocytes (Fig. 9, *D* and *E*). These results may document the importance of phosphorylation of Nephrin and phosphorylation and plasma membrane translocation of PLC-γ1 in injured podocytes *in vivo*.

DISCUSSION

In most of the clinical settings characterized by proteinuria, such as idiopathic nephrotic syndrome, focal segmental glomerulosclerosis, or diabetic nephropathy, the characteristic change in podocyte shape called effacement of foot processes is a common occurrence (1). This change is caused by various damages to podocytes, including mechanical stress, high glucose concentration, reactive oxygen species, or TGF-β (29). Importantly, podocyte can also be damaged by many Ca^{2+}-stimulating vasoactive hormones, including angiotensin II, bradykinin, or endothelin (30). Clinical (31–33) and experimental studies (34–36) suggest that the activation by vasoactive hormones alters the glomerular ultrafiltration coefficient by Ca^{2+}- and cAMP-dependent signals and contributes to the pathogenesis of renal failure. But so far, the mechanism of how podocytes respond to injury or damage is largely unknown.

In this study, we have shown that phosphorylation of Nephrin Tyr-1204 is directly linked to Ca^{2+} signaling via binding to PLC-γ1. Clustering of Nephrin induces phosphorylation of Tyr-1204, which provides a binding site for PLC-γ1. The binding of PLC-γ1 to Nephrin Tyr-1204 induces rapid and sustained phosphorylation of PLC-γ1. Clustering of Nephrin also triggers Ca^{2+} mobilization through PLC-γ1. These results are likely to be relevant to pathogenesis of proteinuria, because

regenerative processes that require feedback elements (42), and the complex temporal and spatial feedback mechanisms are now being revealed (43). Although the precise feedback element that drives the initial phase of Ca^{2+} response remains unclear, a recent study using fluorescent IP_3 sensors revealed that threshold $[IP_3]$ is not constant, rather implying the importance of the IP_3 receptor sensitivity for Ca^{2+} spike generation (44). The time interval between the activation of PLC-γ1 and the $[Ca^{2+}]_i$ rise in our system might be explained by complex feedback mechanisms downstream of signal intensity and PLC activity that modulate the threshold for the Ca^{2+} response.

The recent finding that mutations in TRPC6 can cause focal segmental glomerulosclerosis also highlights the importance of Ca^{2+} signaling in podocyte biology (15). Electrophysiological studies revealed that some mutations of TRPC6 found in patients showed augmented Ca^{2+} influx (15, 16). TRPC6 is also up-regulated in Nephrin-deficient mice or even in human proteinuric kidney diseases (16, 45). These results suggest that an exaggerated Ca^{2+} signal may disrupt glomerular cell function and is a common feature in the pathology of proteinuric diseases. Because TRPC6 has been reported to be structurally and functionally associated with the SD (16, 46), it seems plausible that the recruitment and activation of PLC-γ1 induced by Nephrin phosphorylation may directly or indirectly activate transient receptor potential channels in podocytes *in vivo*.

It is of note that Nck and PLC-γ share the same tyrosine-phosphorylated residue, Tyr-1204 of Nephrin, although Nck also binds to another residue (Tyr-1228 in rat). Phosphorylation-dependent recruitment of Nck is already shown to be necessary for Nephrin-directed actin polymerization. Intriguingly, a recent report has documented a direct link between PLC-γ and actin polymerization via activation of cofilin, a widely distributed actin-modulating protein (47). Cofilin is activated by hydrolysis of phosphatidylinositol 4,5-bisphosphate by PLC-γ, which leads to an asymmetric distribution of cofilin activity, setting the direction of lamellipodium formation and subsequent migration (48). These results raise an interesting possibility that Nephrin regulates actin dynamics by several pathways through binding with various proteins.

Hinkes *et al.* (49) reported that mutations in PLC-ε1 cause congenital nephrotic syndrome; however, the molecular mechanism of pathogenesis is largely unknown. Because PLC-ε1 does not have an SH2 domain, PLC-ε1 will not be directly recruited to phosphorylated Nephrin in a manner similar to PLC-γ1. However, various receptor stimuli seem to engage the activities of multiple PLC subtypes through the action of non-receptor tyrosine kinases, phosphatidylinositol 3-kinase, or Ca^{2+} signals (50). It would be highly valuable to investigate the effect of each PLC signaling pathway on podocyte morphology and viability to understand the mechanism of pathogenesis of proteinuria.

In summary, we identified a posphorylation-dependent interaction between Nephrin and PLC-γ1. We also provide a model system in which Nephrin phosphorylation triggers Ca^{2+} response through the recruitment and activation of PLC-γ1. Given the profound effect of PLC-γ in diverse cellular functions, the role of Nephrin phosphorylation and activation of PLC-γ1 may be important in modulating the function of the glomerular filtration barrier elaborated by differentiated podocytes. These findings also highlight the importance of Ca^{2+} signaling in podocyte biology, and the ability of the podocyte to precisely regulate $[Ca^{2+}]_i$ level may play a critical role in glomerular disease processes.

REFERENCES

1. Pavenstadt, H., Kriz, W., and Kretzler, M. (2003) *Physiol. Rev.* **83,** 253–307
2. Tryggvason, K., Patrakka, J., and Wartiovaara, J. (2006) *N. Engl. J. Med.* **354,** 1387–1401
3. Kestila, M., Lenkkeri, U., Mannikko, M., Lamerdin, J., McCready, P., Putaala, H., Ruotsalainen, V., Morita, T., Nissinen, M., Herva, R., Kashtan, C. E., Peltonen, L., Holmberg, C., Olsen, A., and Tryggvason, K. (1998) *Mol. Cell* **1,** 575–582
4. Putaala, H., Soininen, R., Kilpelainen, P., Wartiovaara, J., and Tryggvason, K. (2001) *Hum. Mol. Genet.* **10,** 1–8
5. Donoviel, D. B., Freed, D. D., Vogel, H., Potter, D. G., Hawkins, E., Barrish, J. P., Mathur, B. N., Turner, C. A., Geske, R., Montgomery, C. A., Starbuck, M., Brandt, M., Gupta, A., Ramirez-Solis, R., Zambrowicz, B. P., and Powell, D. R. (2001) *Mol. Cell. Biol.* **21,** 4829–4836
6. Roselli, S., Heidet, L., Sich, M., Henger, A., Kretzler, M., Gubler, M. C., and Antignac, C. (2004) *Mol. Cell. Biol.* **24,** 550–560
7. Ciani, L., Patel, A., Allen, N. D., and Ffrench-Constant, C. (2003) *Mol. Cell. Biol.* **23,** 3575–3582
8. Shih, N. Y., Li, J., Karpitskii, V., Nguyen, A., Dustin, M. L., Kanagawa, O., Miner, J. H., and Shaw, A. S. (1999) *Science* **286,** 312–315
9. Benzing, T. (2004) *J. Am. Soc. Nephrol.* **15,** 1382–1391
10. Huber, T. B., Hartleben, B., Kim, J., Schmidts, M., Schermer, B., Keil, A., Egger, L., Lecha, R. L., Borner, C., Pavenstadt, H., Shaw, A. S., Walz, G., and Benzing, T. (2003) *Mol. Cell. Biol.* **23,** 4917–4928
11. Verma, R., Wharram, B., Kovari, I., Kunkel, R., Nihalani, D., Wary, K. K., Wiggins, R. C., Killen, P., and Holzman, L. B. (2003) *J. Biol. Chem.* **278,** 20716–20723
12. Verma, R., Kovari, I., Soofi, A., Nihalani, D., Patrie, K., and Holzman, L. B. (2006) *J. Clin. Invest.* **116,** 1346–1359
13. Jones, N., Blasutig, I. M., Eremina, V., Ruston, J. M., Bladt, F., Li, H., Huang, H., Larose, L., Li, S. S., Takano, T., Quaggin, S. E., and Pawson, T. (2006) *Nature* **440,** 818–823
14. Yu, C. C., Yen, T. S., Lowell, C. A., and DeFranco, A. L. (2001) *Curr. Biol.* **11,** 34–38
15. Winn, M. P., Conlon, P. J., Lynn, K. L., Farrington, M. K., Creazzo, T., Hawkins, A. F., Daskalakis, N., Kwan, S. Y., Ebersviller, S., Burchette, J. L., Pericak-Vance, M. A., Howell, D. N., Vance, J. M., and Rosenberg, P. B. (2005) *Science* **308,** 1801–1804
16. Reiser, J., Polu, K. R., Moller, C. C., Kenlan, P., Altintas, M. M., Wei, C., Faul, C., Herbert, S., Villegas, I., Avila-Casado, C., McGee, M., Sugimoto, H., Brown, D., Kalluri, R., Mundel, P., Smith, P. L., Clapham, D. E., and Pollak, M. R. (2005) *Nat. Genet.* **37,** 739–744
17. Dowden, J., Berridge, G., Moreau, C., Yamasaki, M., Churchill, G. C., Potter, B. V., and Galione, A. (2006) *Chem. Biol.* **13,** 659–665
18. Tezuka, T., Umemori, H., Akiyama, T., Nakanishi, S., and Yamamoto, T. (1999) *Proc. Natl. Acad. Sci. U. S. A.* **96,** 435–440
19. Bae, S. S., Perry, D. K., Oh, Y. S., Choi, J. H., Galadari, S. H., Ghayur, T., Ryu, S. H., Hannun, Y. A., and Suh, P. G. (2000) *FASEB J.* **14,** 1083–1092
20. Yamasaki, S., Ishikawa, E., Sakuma, M., Ogata, K., Sakata-Sogawa, K., Hiroshima, M., Wiest, D. L., Tokunaga, M., and Saito, T. (2006) *Nat. Immunol.* **7,** 67–75
21. Harita, Y., Kurihara, H., Kosako, H., Tezuka, T., Sekine, T., Igarashi, T., and Hattori, S. (2008) *J. Biol. Chem.* **283,** 9177–9186

22. Nagai, T., Sawano, A., Park, E. S., and Miyawaki, A. (2001) *Proc. Natl. Acad. Sci. U. S. A.* **98,** 3197–3202

23. Hirabayashi, S., Mori, H., Kansaku, A., Kurihara, H., Sakai, T., Shimizu, F., Kawachi, H., and Hata, Y. (2005) *Lab. Invest.* **85,** 1528–1543

24. Poulin, B., Sekiya, F., and Rhee, S. G. (2005) *Proc. Natl. Acad. Sci. U. S. A.* **102,** 4276–4281

25. Fliegert, R., Gasser, A., and Guse, A. H. (2007) *Biochem. Soc. Trans.* **35,** 109–114

26. Galione, A. (2006) *Biochem. Soc. Trans.* **34,** 922–926

27. Kurihara, H., Anderson, J. M., and Farquhar, M. G. (1995) *Am. J. Physiol.* **268,** F514–F524

28. Garg, P., Verma, R., Nihalani, D., Johnstone, D. B., and Holzman, L. B. (2007) *Mol. Cell. Biol.* **27,** 8698–8712

29. Shankland, S. J. (2006) *Kidney Int.* **69,** 2131–2147

30. Pavenstadt, H. (2000) *Am. J. Physiol. Renal Physiol.* **278,** F173–F179

31. Maschio, G., Alberti, D., Janin, G., Locatelli, F., Mann, J. F., Motolese, M., Ponticelli, C., Ritz, E., and Zucchelli, P. (1996) *N. Engl. J. Med.* **334,** 939–945

32. Ruggenenti, P., Perna, A., Gherardi, G., Garini, G., Zoccali, C., Salvadori, M., Scolari, F., Schena, F. P., and Remuzzi, G. (1999) *Lancet* **354,** 359–364

33. Brenner, B. M., Cooper, M. E., de Zeeuw, D., Keane, W. F., Mitch, W. E., Parving, H. H., Remuzzi, G., Snapinn, S. M., Zhang, Z., and Shahinfar, S. (2001) *N. Engl. J. Med.* **345,** 861–869

34. Lafayette, R. A., Mayer, G., Park, S. K., and Meyer, T. W. (1992) *J. Clin. Invest.* **90,** 766–771

35. Remuzzi, A., Perico, N., Amuchastegui, C. S., Malanchini, B., Mazerska, M., Battaglia, C., Bertani, T., and Remuzzi, G. (1993) *J. Am. Soc. Nephrol.* **4,** 40–49

36. Benigni, A., Tomasoni, S., Gagliardini, E., Zoja, C., Grunkemeyer, J. A., Kalluri, R., and Remuzzi, G. (2001) *J. Am. Soc. Nephrol.* **12,** 941–948

37. Patterson, R. L., van Rossum, D. B., Ford, D. L., Hurt, K. J., Bae, S. S., Suh, P. G., Kurosaki, T., Snyder, S. H., and Gill, D. L. (2002) *Cell* **111,** 529–541

38. Tu, C. L., Chang, W., and Bikle, D. D. (2005) *J. Invest. Dermatol.* **124,** 187–197

39. Litjens, T., Nguyen, T., Castro, J., Aromataris, E. C., Jones, L., Barritt, G. J., and Rychkov, G. Y. (2007) *Biochem. J.* **405,** 269–276

40. van Rossum, D. B., Patterson, R. L., Sharma, S., Barrow, R. K., Kornberg, M., Gill, D. L., and Snyder, S. H. (2005) *Nature* **434,** 99–104

41. Broad, L. M., Braun, F. J., Lievremont, J. P., Bird, G. S., Kurosaki, T., and Putney, J. W., Jr. (2001) *J. Biol. Chem.* **276,** 15945–15952

42. Meyer, T., and Stryer, L. (1991) *Annu. Rev. Biophys. Biophys. Chem.* **20,** 153–174

43. Brandman, O., and Meyer, T. (2008) *Science* **322,** 390–395

44. Matsu-ura, T., Michikawa, T., Inoue, T., Miyawaki, A., Yoshida, M., and Mikoshiba, K. (2006) *J. Cell Biol.* **173,** 755–765

45. Moller, C. C., Wei, C., Altintas, M. M., Li, J., Greka, A., Ohse, T., Pippin, J. W., Rastaldi, M. P., Wawersik, S., Schiavi, S., Henger, A., Kretzler, M., Shankland, S. J., and Reiser, J. (2007) *J. Am. Soc. Nephrol.* **18,** 29–36

46. Huber, T. B., Schermer, B., Muller, R. U., Hohne, M., Bartram, M., Calixto, A., Hagmann, H., Reinhardt, C., Koos, F., Kunzelmann, K., Shirokova, E., Krautwurst, D., Harteneck, C., Simons, M., Pavenstadt, H., Kerjaschki, D., Thiele, C., Walz, G., Chalfie, M., and Benzing, T. (2006) *Proc. Natl. Acad. Sci. U. S. A.* **103,** 17079–17086

47. Kolsch, V., Charest, P. G., and Firtel, R. A. (2008) *J. Cell Sci.* **121,** 551–559

48. Ghosh, M., Song, X., Mouneimne, G., Sidani, M., Lawrence, D. S., and Condeelis, J. S. (2004) *Science* **304,** 743–746

49. Hinkes, B., Wiggins, R. C., Gbadegesin, R., Vlangos, C. N., Seelow, D., Nurnberg, G., Garg, P., Verma, R., Chaib, H., Hoskins, B. E., Ashraf, S., Becker, C., Hennies, H. C., Goyal, M., Wharram, B. L., Schachter, A. D., Mudumana, S., Drummond, I., Kerjaschki, D., Waldherr, R., Dietrich, A., Ozaltin, F., Bakkaloglu, A., Cleper, R., Basel-Vanagaite, L., Pohl, M., Griebel, M., Tsygin, A. N., Soylu, A., Muller, D., Sorli, C. S., Bunney, T. D., Katan, M., Liu, J., Attanasio, M., O'Toole J, F., Hasselbacher, K., Mucha, B., Otto, E. A., Airik, R., Kispert, A., Kelley, G. G., Smrcka, A. V., Gudermann, T., Holzman, L. B., Nurnberg, P., and Hildebrandt, F. (2006) *Nat. Genet.* **38,** 1397–1405

50. Rebecchi, M. J., and Pentyala, S. N. (2000) *Physiol. Rev.* **80,** 1291–1335